

## Supporting Information

### Total energy minimization

In our model, all the tubes are assumed straight initially and the nanotube structural distortion at crossed junctions are considered. The geometric configuration at junction is determined by minimizing a constrained total energy. In that process, the position of the atoms near the junction is fully relaxed while the center-to-center tube distance ( $d$ ) is fixed. If  $d$  is smaller than the CNT diameter ( $D$ ) plus the van der Waals distance ( $d_{vdw}$ ), the tube wall will bend to avoid either penetrating each other or underestimating tube-tube interaction. The total pseudo potential energy ( $E$ ) of the junction can be expressed by  $E = 2E_b + E_{LJ}$ , where  $E_b$  is the energy associated with the bending of CNT walls and  $E_{LJ}$  is the Lenard–Jones (L-J) potential associated with the van der Waals interaction between CNTs, respectively. The local structural distortions of CNTs and the separation gap between two distorted CNT walls are determined self-consistently by minimizing the total energy.

Assume the energy associated with the bending of CNT wall can be represented by a harmonic potential as

$$E_s = \frac{1}{2}k_s (D - D')^2 \quad (\text{S1})$$

where  $D$  is the diameter of CNT before distortion,  $D'$  is the nominal diameter of distorted CNT,  $k_s$  is the equivalent spring constant of CNT wall. The spring constant can be derived from the atomic dynamic simulations by keeping one CNT fixed, while

slowly moving another CNT towards the fixed one in the radial direction. As two CNTs are radially compressed, we can calculate the force-deformation curve by the coarse-grained molecular dynamic model and derive the spring constant  $k_s$ .

The potential energy associated with the van der Waals interaction is represented by the Lennard-Jones potential,

$$E_v = 4k_v \left[ \left( \frac{\sigma}{d_{gap}} \right)^{12} - \left( \frac{\sigma}{d_{gap}} \right)^6 \right] \quad (S2)$$

where  $k_v$  is the depth of the potential well obtained from the atomic dynamic model,  $\sigma$  is the finite distance at which the potential is zero.

Results show that the separation gap in an effective contact region of two CNTs reaches an extreme at nearly 0.26 nm. Any further decrease in the distance  $d$  will bend the CNT walls over a larger area rather than decrease the gap between CNT walls.

### **Parametric studies**

Here, the effects of CNT morphology, electrical properties and TCR of CNTs, work function of polymer on the TCR properties of CNT/polymer composites are investigated. At first, the effects of TCR of CNTs on the electrical conductivity and resistance change ratio of CNT/polymer composites are shown in Figure S1. The TCR of CNT varying from 10 to 100, while the remaining parameters are kept the same. The

simulation results reveal a limited decrease of resistance change ratio as the TCR of CNT increases.

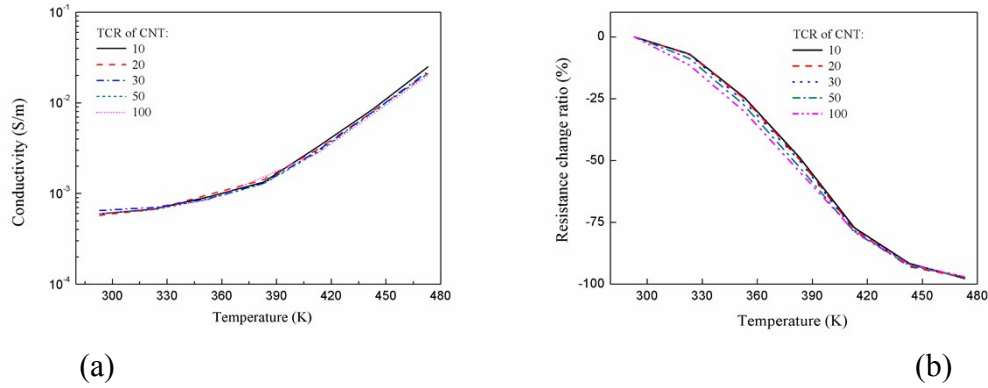
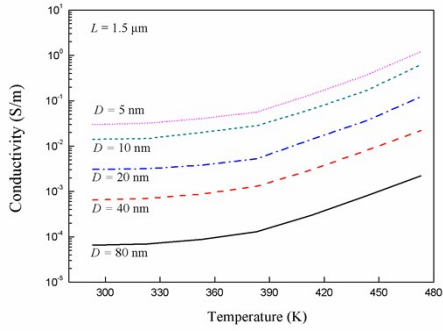
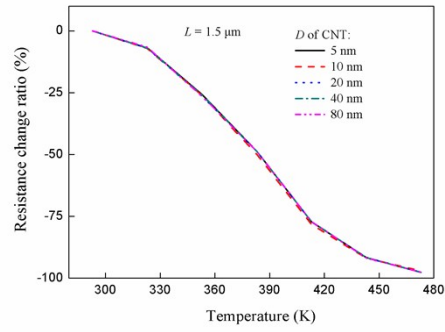


Figure S1. Effect of TCR of CNT on electrical conductivity (a) and resistance change ratio (b) of CNT/polymer composites as temperature ranging from 293 K to 473 K.

Next, Monte Carlo simulations are conducted for CNT diameter from 5 nm to 80 nm at a fixed CNT lengths of 1.5  $\mu\text{m}$ . This is equivalent to the aspect ratio ranging from 18 to 300. The simulation results in Figure S2 reveal that the electrical conductivity increases steadily as the CNT aspect ratio increases. It indicates that the large CNT aspect ratio increases the probability to form CNT junctions in the polymer matrix to reduce the overall resistance. However, the resistance change ratio of CNT/polymer composite is almost independent of CNT morphology.



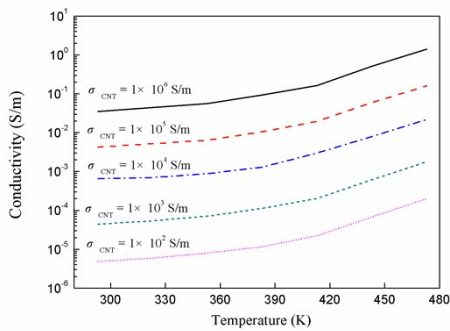
(a)



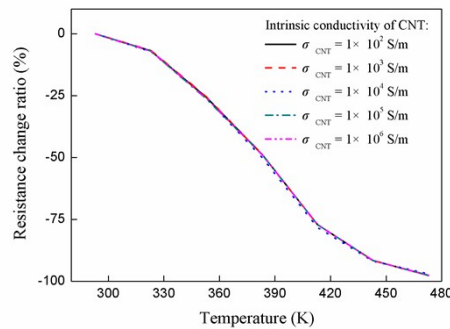
(b)

Figure S2. Effect of CNT morphology on electrical conductivity (a) and resistance change ratio (b) of CNT/polymer composites as temperature ranging from 293 K to 473 K.

Then, simulations are conducted for the CNT intrinsic conductivity varying from  $10^3$  to  $10^6$  S/m, which is the typical range of intrinsic conductivity reported experimentally for MWCNTs. It shows in Figure S3 that the electrical conductivity is enhanced substantially as the CNT intrinsic conductivity increases. Once again, the resistance change ratio of CNT/polymer composite is also not sensitive to CNT intrinsic conductivity.



(a)



(b)

Figure S3. Effect of CNT intrinsic conductivity on electrical conductivity (a) and resistance change ratio (b) of CNT/polymer composites as temperature ranging from 293 K to 473 K.

Finally, the effects of work functions of polymer matrix on the electrical conductivity and resistance change ratio are studied and shown in Figure S4. The polymers' work functions vary from 3.25 to 4.5 eV, with the typical values for nylon 66, polystyrene, polycarbonate, and polyimide are 3.95 eV, 4.22 eV, 4.26 eV, and 4.36 eV, respectively. Simulation results show that the polymer's work functions have limited effects on both electrical conductivity and resistance change ratio of CNT/polymer composite.

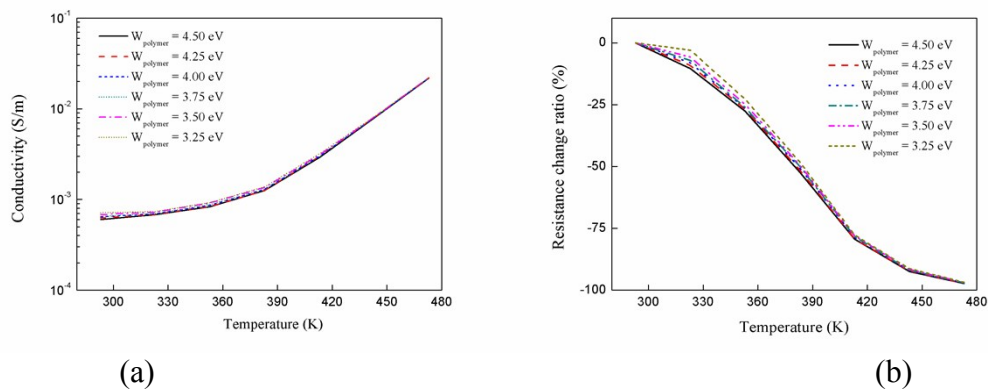


Figure S4. Effect of work function of polymer matrix on electrical conductivity (a) and resistance change ratio (b) of CNT/polymer composites as temperature ranging from 293 K to 473 K.